



Myocardial ischemia and right ventricular dysfunction in adult patients with sickle cell disease

Subha V. Raman
Orlando P. Simonetti
Spero R. Cataland
Eric H. Kraut

Background and Objectives. Patients with sickle cell disease (SCD) have multi-organ manifestations of microvascular disease, though cardiac manifestations have been poorly characterized *in vivo*. This study sought to characterize myocardial characteristics in adult patients with SCD.

Design and Methods. Twenty-two consecutive outpatients and 11 age-matched controls underwent magnetic resonance imaging to assess myocardial perfusion reserve as well as left and right ventricular size and function and myocardial iron. Computed tomography of the coronary arteries was performed to assess epicardial coronary stenosis.

Results. Three of 22 outpatients with clinically stable SCD and no controls had abnormal myocardial perfusion reserve limited to the subendocardium, consistent with microvascular disease. Coronary arteries were free of disease as detectable by computed tomography angiography. Myocardial T2* was normal in all subjects (29 ± 5 ms, median 29ms), consistent with absence of cardiac iron deposition despite a high prevalence of hepatic iron overload (liver T2* 14 ± 9 ms, median 12.0ms). SCD patients had right ventricular enlargement and dysfunction (right ventricular ejection fraction 45 ± 15 in SCD patients vs. $58 \pm 5\%$ in controls, $p=0.001$) even in the absence of overt pulmonary hypertension.

Interpretation and Conclusions. A subset of adult SCD patients may have myocardial ischemia in the absence of infarcted myocardium, myocardial iron overload, or coronary artery disease. Right ventricular dysfunction is present in stable SCD patients, despite normal resting pulmonary artery pressures. These findings could represent under-recognized mechanisms for chest pain and mortality in this population, and warrant further investigation in SCD crises.

Key words: sickle cell disease, myocardial ischemia, right ventricle

Haematologica 2006; 91:1329-1335

©2006 Ferrata Storti Foundation

From the Department of Internal Medicine, Divisions of Cardiovascular Medicine (SVR, OPS) and Hematology (SRC, EHK), Ohio State University, Columbus, USA.

Correspondence:

Subha V. Raman, MD, Assistant Professor, Division of Cardiovascular Medicine, The Ohio State University 473 W. 12th Avenue, Suite 200 Columbus, OH 43210 USA.
E-mail: Raman.1@osu.edu

Sickle cell disease (SCD) affects millions of people of various ethnicities around the world, with protean clinical manifestations due to vascular occlusion by sickled red blood cells.^{1,2} Case series have also identified a spectrum of cardiac complications including ischemia, left ventricular hypertrophy, and heart failure. Myocardial infarction also occurs as previously described in isolated case reports.^{3,4} Historically, nuclear scintigraphic imaging using isotopes such as thallium have been used to detect myocardial perfusion abnormalities in children with SCD, although reduced sensitivity to detect subendocardial myocardial perfusion abnormalities may have limited the utility of such techniques in adequately identifying myocardial disease in SCD patients. Recent advances in magnetic resonance perfusion imaging have allowed *in vivo* identification of microvascular disease which cannot be appreciated with nuclear techniques, in other populations⁵. Recognition of myocardial ischemia in SCD patients would motivate more aggressive use of cardiovascular therapeutics that have proven to be effective

in reducing symptoms and acute events in other populations with ischemic heart disease.^{6,7} We sought to characterize the myocardium of adult patients with SCD using a comprehensive noninvasive diagnostic strategy.

Design and Methods

Study population

We prospectively recruited 22 patients from the Adult Comprehensive Sickle Cell Program of the Ohio State University, which includes both tertiary care and community sites. Criteria for inclusion consisted of SCD documented by hemoglobin electrophoresis and age ≥ 18 years. Patients were excluded from enrollment if they had any of the following contraindications to magnetic resonance examination: ferromagnetic metal anywhere in the body, severe claustrophobia, or an active implant such as a pacemaker or neurostimulator. Additional study exclusion criteria included: transfusion requirement over the preceding 8 weeks to

Table 1. Clinical characteristics of sickle cell patients. Patients with myocardial ischemia are highlighted in bold.

Subject No.	Age (years)	Sex	HBE	Mean Hb	Xfn	RVSP	CP	Hydroxyurea	Ulcers/Priapism	LDH (U/L)	Ferritin (ng/mL)	Irreversibly sickled cells	Myo T2*	Liver T2*	Ischemia
1	20	F	SS	11.4	Y	21	N	Y	N	316	267	1+	27	33	N
2	27	F	SS	9.9	Y	21	N	N	N	233	576	1+	26	5.0	N
3	31	F	SS	7.5	Y	34	Y	N	N	129	>1000	2+	32	3.5	N
4	20	M	SS	6.9	Y	41	N	Y	N	423	>1000	2+	33	12.0	adenosine stopped due to dyspnea perfusion not completed due to AF w/RVR
5	45	M	SS	7.0	Y	73	N	N	Y	1103	551	2+	25	18.3	N
6	25	F	S-thal	9.4	N	N/A	Y	N	N	N/A	753	0	24	6.7	N
7	20	F	SS	8.7	Y	N/A	N	N	N	282	>1000	1+	27	3.7	SE Ischemia
8	41	M	SS	5.3	Y	21	N	N	N	434	>1000	3+	37	7.1	SE Ischemia
9	25	M	SC	14.8	N	N/A	Y	N	Y	N/A	189	0	36	26.0	N
10	25	F	SS	8.9	Y	33	N	N	N	429	765	2+	29	11.0	N
11	22	M	SS-IF	12.6	Y	N/A	N	Y	N	462	253	0	n/a	n/a	n/a
12	21	F	SS	7.8	N	21	Y	N	N	N/A	53	1+	33	23.0	SE ischemia
13	33	F	SC	8.3	Y	37	N	N	N	238	958	2+	22	8.0	N
14	47	M	SS	8.9	Y	23	Y	N	N	190	169	1+	22	21.0	N
15	28	F	SS	11.3	Y	21	Y	Y	N	334	n/a	2+	34	24.0	N
16	31	F	SS	8.2	Y	N/A	Y	N	N	316	>1000	2+	32	6.0	n/a
17	27	F	S-thal	7.4	Y	34	N	N	N	538	491	1+	32	16.0	P
18	36	M	SC	13.3	Y	N/A	Y	N	N	514	94	0	28	28.0	N
19	21	M	SS	7.7	Y	30	N	N	N	N/A	>1000	1+	32	2.0	N/A
20	35	F	SS	8.6	Y	33	N	N	N	316	>1000	3+	33	5.5	N
21	19	F	SS	9.1	Y	N/A	N	N	N	233	591	1+	21	16.0	N
22	28	F	SS-IF	8.2	Y	30	N	N	N	129	116	2+	26	25.0	N

HBE: hemoglobin electrophoresis; Hb: hemoglobin; Xfn: transfusion; RVSP: right ventricular systolic pressure; CP: chest pain; Myo: myocardial; LDH: serum lactate dehydrogenase level in IU/L; AF: atrial fibrillation; RVR: rapid ventricular response; SS-IF: SS with increased hemoglobin F; N/A: not available.

maintain hemoglobin levels ≥ 6 mg/dL, monthly exchange transfusions, creatinine above 1.5 mg/dL, history of allergy to radiocontrast agents, pregnancy, active use of calcium channel blockers or nitrates, and a documented history of epicardial coronary artery disease. Each subject was assessed by one of the investigators to document the presence of any cardiovascular signs and symptoms as well as a history of cardiovascular events, and all subjects underwent routine 12-lead surface electrocardiography. Two patients had pulmonary hypertension confirmed by invasive pressure measurement; in the remaining subjects, right ventricular systolic pressure was calculated from absolute tricuspid regurgitation velocity on echocardiograph using the well-established Bernoulli formula (Table 1).⁸ All patients gave written informed consent to participate in this Institutional Review Board-approved protocol.

Cardiac magnetic resonance examination

The cardiac magnetic resonance examination was completed on a standard clinical 1.5 Tesla magnetic resonance scanner (MAGNETOM Avanto, Siemens Medical Solutions, Inc., Erlangen, Germany) equipped with the necessary hardware and software to perform cardiovascular imaging. The protocol included: horizontal long-axis, vertical long-axis, and three-chamber long-axis and contiguous short-axis cine true-FISP acquisitions for the measurement of right and left ventricular

volumes, mass and ejection fraction. Myocardial T2*, a relaxation parameter that is directly related to myocardial iron content,⁹ was measured in a single mid-short axis slice using an ECG-triggered, segmented, multiple-echo, gradient-echo acquisition with echo times of 1.22, 2.64, 4.59, 7.56, 11.1, 15.0, 18.9, 22.8, and 26.7 ms. Using the images from all nine echo times, a region of interest was defined in the inter-ventricular septum and a mono-exponential decay curve was fit to compute myocardial T2*. Myocardial perfusion was imaged at rest and during intravenous administration of adenosine according to standard protocols.¹⁰ Subjects received 140 mcg/kg of adenosine over 4 minutes with simultaneous acquisition of multislice stress perfusion images using 0.075 mmol/kg IV gadolinium-DTPA (Omniscan, GE Healthcare, Waukesha, WI, USA) which was repeated at rest allowing 15 minutes to elapse after acquisition of the stress perfusion images. Late post-gadolinium enhancement (LGE) imaging was performed 5-10 minutes after final contrast administration in the horizontal long-axis, vertical long-axis, three-chamber long-axis, and multislice short-axis planes to identify any myocardial infarct scar. Perfusion acquisition employed a hybrid gradient echo – echo planar (GRE-EPI) technique with adaptive sensitivity encoding (TSENSE).¹¹ Perfusion defects were visually identified as present or absent based on lack of contrast-enhancement of the myocardium. LGE imaging was performed 5-10 min-

utes after final contrast administration in the horizontal long-axis, vertical long-axis, three-chamber long-axis, and multi-slice short-axis planes to identify any myocardial infarct scar. The LGE acquisition was carried out using a T1-weighted inversion-recovery gradient echo sequence,¹² optimizing the inversion time for adequate myocardial suppression and scar visualization. LGE images were reviewed for the presence and location of myocardial scars. All image reviews were performed blinded to the subject's history.

Computed tomography examination

The computed tomography examination was performed on a 64-slice scanner (SOMATOM Sensation⁶⁴, Siemens Medical Solutions, Inc., Forchheim, Germany) scanner. Oral or intravenous β -blockade was administered at the onset of the examination if the heart rate exceeded 70 beats per minute. Non-contrast axial sections through the heart (3 mm) were obtained for calcium scoring. A low-volume contrast timing bolus scan using 20 mL of intravenous isosmolar contrast agent (Visipaque, GE Healthcare, Waukesha, WI, USA) was run. From this scan, a region of interest was drawn in the ascending aorta to derive a signal-intensity vs. time curve, from which the time of contrast arrival in the aortic root was determined. Using this delay, a contrast-enhanced helical scan covering the heart was performed. Detector collimation was 32×0.6 mm resulting in 64 slices per rotation with an overlap of 0.3 mm, and reconstructed slice resolution of approximately 0.4 mm.¹³ The gantry rotation speed was 330 ms per rotation and the tube voltage was 120 Kv with application of electrocardiographically-guided dose modulation to reduce the tube current by 80% during the systolic phases of the cardiac cycle. Image data were acquired with inspiratory breathholding (10-12 seconds depending on heart rate) during injection of 80 cc of contrast agent at a rate of 5 cc/sec followed by injection of a 20 cc saline flush at a rate of 5 cc/sec. Electrocardiographically-gated data sets were reconstructed at end-diastole. Timing was adjusted and additional reconstructions generated if motion artifacts were present. The resulting thin sections were reviewed in axial sections as well as multiplanar reformatted images to visualize each segment of the coronary tree. All image reviews were performed blinded to the subject's history.

Statistical analysis

Data are expressed as means \pm standard deviation. Differences between means of continuous variables were tested by Wilcoxon non-parametric tests. The χ^2 test was used to compare categorical data. A p value of less than 0.05 was considered to be statistically significant.

Role of the funding source

The sponsors of the study had no role in study design, data collection, data analysis, data interpretation, or writing of the report.

Results

Clinical characteristics

The baseline characteristics of all patients and age-matched controls are shown in Table 1. No patients evaluated for enrollment had known epicardial coronary artery disease. The genotype based on hemoglobin electrophoresis was hemoglobin SS in 19 patients (86%), hemoglobin SC in two (9%) and hemoglobin S-thalassemia in one (5%). Average hemoglobin in the preceding 3 months for sickle cell (SS) patients was 9 ± 2 mg/dL with higher values being recorded in the SC patients. Lactate dehydrogenase levels were available in 16 subjects, and ranged from 129 to 1103 IU/L, the highest value recorded in a patient with end-stage pulmonary hypertension.

Serum ferritin ranged from 53 to >1000 ng/mL. Only one patient (n. 21) was on chelation therapy at the time of participation in the study. Eight patients reported chest pain as a complication of their SCD. Electrocardiography demonstrated sinus tachycardia (n=7) sinus rhythm (n=8), sinus bradycardia (n=2), and atrial fibrillation (n=1).

Myocardial characteristics

Three SS patients had abnormal subendocardial perfusion based on absent gadolinium-enhancement of the subendocardial myocardium during perfusion imaging with vasodilator stress which was not present in controls (Figure 1). In a fourth patient, adenosine perfusion was prematurely terminated due to chest pain precluding imaging assessment of ischemia. Overall, 11 (50%) patients experienced chest pain following infusion of adenosine; no significant hypotension occurred. No significant electrocardiographic changes occurred with the adenosine infusions. None of the patients or controls had evidence of prior myocardial infarction by late post-gadolinium enhancement imaging. Despite frequent transfusions in many of the patients, measurement of T2* in the myocardium was normal (median 29 ms), consistent with the absence of myocardial iron overload. Liver T2* was <20 ms in 14 SCD patients (median 12 ms for all SCD patients) consistent with significant hepatic iron overload (Figure 2).

Ventricular size and function

Compared to controls, sickle cell patients had higher left ventricular (LV) volumes (LV end-diastolic volume index 88 ± 26 mL/m² in SCD vs. 71 ± 18 in controls, $p=0.05$) but preserved systolic function (LV ejection fraction $58\pm 6\%$ in SCD vs. $60\pm 8\%$ in controls, $p=NS$). Right

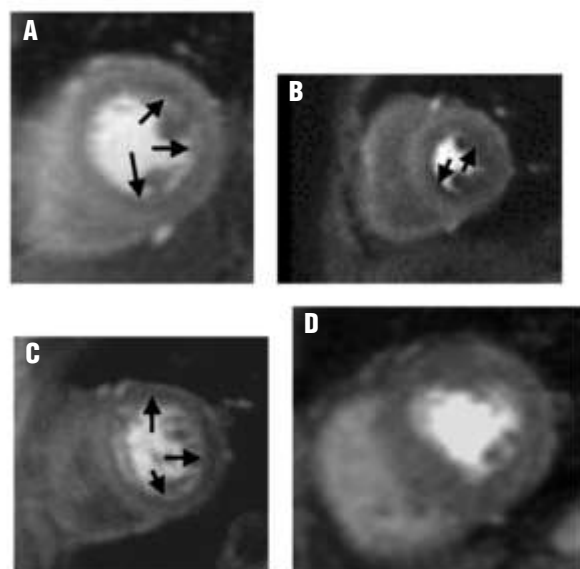


Figure 1. Abnormal subendocardial perfusion seen as a rim of hypoenhancement (A-C, arrows) on gadolinium-enhanced T1-weighted imaging during first-pass acquisition in three sickle cell patients and a patient with normal myocardial perfusion (D).

ventricular (RV) size was increased (RV end-diastolic volume index 84 ± 25 mL/m² in SCD vs. 59 ± 9 mL/m² in controls, $p=0.001$), with RV systolic function being poorer in sickle cell patients than in controls (RV ejection fraction $45 \pm 15\%$ in SCD vs. $58 \pm 5\%$ in controls, $p=0.001$). Absolute RV systolic pressure calculated from the tricuspid regurgitation velocity, which is equivalent to pulmonary artery systolic pressure in the absence of pulmonary stenosis, correlated significantly with RV ejection fraction ($p=0.01$). Cardiac measurements are summarized in Table 2.

Coronary arteries

Visualization of the entire coronary tree was excellent using multidetector row computed tomography angiography, and showed normal epicardial coronary arteries in all subjects. The calcium score was zero in all subjects.

Subgroup analysis

The three subjects with microvascular ischemia tended to have lower mean hemoglobin levels than the 19 subjects without myocardial ischemia (7.3 ± 1.0 mg/dL vs. 9.4 ± 0.5 mg/dL, $p=0.06$). Serum lactate dehydrogenase levels, liver T2*, and a history of transfusion did not predict the presence of myocardial ischemia ($p=NS$). There was also no significant difference in the number of hydroxyurea therapy recipients in ischemic (0 of 3) vs. non-ischemic subjects (4 of 19), though the prevalence rates were small.

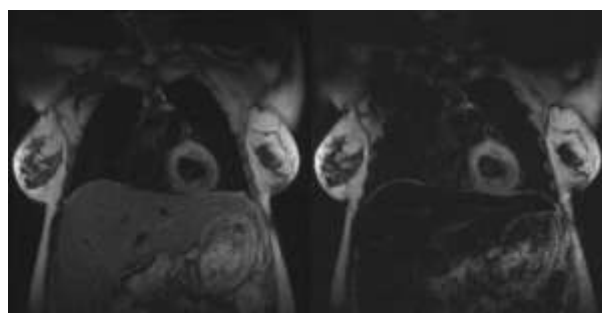


Figure 2. T2*-weighted dark blood imaging obtained in the coronal plane at short (left) and long (right) echo times in a sickle cell patient. Note the suppression of signal from the liver indicating hepatic iron overload. The myocardium retains its signal at longer echo times, consistent with absence of myocardial iron deposition.

Table 2. Cardiac structure and function in patients with sickle cell disease and control subjects.

Variable	Patients		Controls		p value
	Total No.	value	Total No.	value	
LVEDVI (mL/m ²)	20	88±26	11	71±18	0.05
LVESVI (mL/m ²)	20	37±12	11	29±10	NS
LVEF (%)	20	58±6	11	60±8	NS
RVEDVI (mL/m ²)	20	84±25	11	59±9	0.001
RVESVI (mL/m ²)	20	46±18	11	25±6	<0.001
RVEF (%)	20	45±15	11	58±5	0.001
Myocardial T2* (ms)	21	29±5	11	30±3	NS
Liver T2* (ms)	21	14±9	11	27±4	<0.001

Values are expressed as mean±SD. Volumes are reported indexed to body surface area. LVEDVI: left ventricular end-diastolic volume index; LVESVI: left ventricular end-systolic volume index; LVEF: left ventricular ejection fraction; RVEDVI: right ventricular end-diastolic volume index; RVESVI: right ventricular end-systolic volume index; RVEF: right ventricular ejection fraction; ms: milliseconds.

Discussion

We found myocardial perfusion abnormalities in stable outpatients with SCD who were not in crisis. This comprehensive investigation in adult patients utilizing state-of-the-art non-invasive techniques for cardiovascular assessment showed that ischemia occurred in the absence of epicardial coronary artery disease or myocardial iron overload. The subendocardial perfusion abnormality, indicative of microvascular disease, was similar to that seen in other patients with conditions such as the metabolic syndrome.⁵ Other potential causes of microvascular disease, including hypertension, diabetes, and metabolic syndrome, were absent in all the sickle cell patients in this study. Obstruction of an epicardial coronary artery in SCD patients has been infrequently reported in the literature, while myocardial infarction in SCD has also been observed in the absence of obstructive coronary artery disease.^{3,4,14-16} Late post-gadolinium imaging, a highly sensitive technique for infarct detection, did not detect any myocardial scarring in this

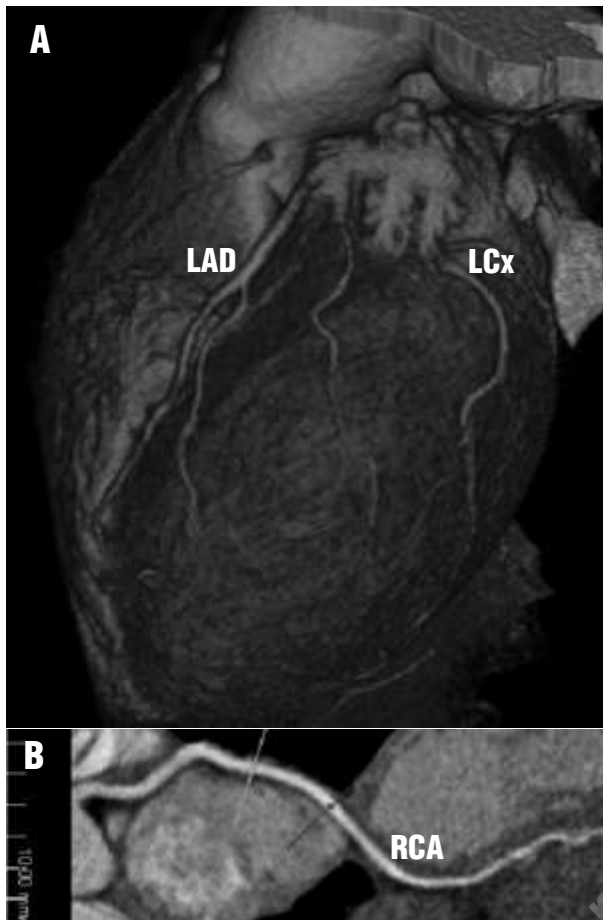


Figure 3. Normal left (A) and right (B) coronary arteries in a patient with sickle cell disease. LAD: left anterior descending; LCx: left circumflex; RCA: right coronary artery.

cohort.¹⁷⁻¹⁹ While the study was not designed to assess myocardial perfusion during crises, the findings suggest that cardiac microvascular abnormalities warrant further consideration as a potential mechanism of chest pain in sickle cell patients. Recognition of myocardial perfusion abnormalities in the acute setting might motivate the use of proven ischemia-relieving therapies, such as nitrates, in addition to the narcotic analgesics typically used to relieve pain in this population. Further investigations utilizing the diagnostic strategies demonstrated in this work are needed to define the prevalence of microvascular cardiac disease in the acute setting. In addition, our findings indicating a trend toward lower hemoglobin levels in patients with ischemia warrant consideration of transfusion to reverse these perfusion abnormalities in sickle cell patients.

Studies using less sensitive measures of myocardial perfusion such as nuclear scintigraphy have documented exercise-induced myocardial ischemia in patients with SCD;²⁰ these techniques also have notoriously higher false positive rates, reducing their specificity. Using thallium-201 single photon emission computed tomography (SPECT), Manoury *et al.* found perfusion abnormalities,

both fixed and reversible, in 14 of 23 SCD patients aged 3 to 19 years.²¹ Acar *et al.*, in a smaller study in children, found perfusion abnormalities by stress thallium-SPECT in three of eight subjects.²² The same group published an extensive clinical investigation including stress thallium-SPECT myocardial perfusion data.²³ They demonstrated that the subjects with perfusion defects were older, had greater number of vasoocclusive crises, and had lower hemoglobin levels compared to eight subjects without myocardial perfusion abnormalities. None of the patients who underwent invasive coronary angiography had obstructive epicardial disease, which is consistent with the results of previous studies including angiography as well as autopsy data.³

Of note, the prevalence of perfusion abnormalities in our study population was lower than the 64% (14 of 22 patients) described by de Montalambert and colleagues despite their use of SPECT-based perfusion techniques which are less sensitive than magnetic resonance-based perfusion imaging. Apart from higher false positives with SPECT perfusion imaging, this may be explained by their considerably younger study population (age 3 to 19 years), suggesting that survival to adulthood occurs in those with nitric oxide or other molecular characteristics (perhaps related to nitric oxide metabolism) that preserve myocardial perfusion whereas those who have less favorable molecular mechanisms to ensure adequate myocardial perfusion reserve die in childhood.

Several authors have found abnormal left ventricular size and function in SCD patients using echocardiography.²⁴⁻²⁶ However, structural changes have not always correlated with physiological abnormalities.²² Given the prevalence of pulmonary hypertension in SCD patients,²⁷ assessment of the right ventricle leveraging cardiac magnetic resonance imaging's proven ability to quantify RV size and systolic function^{28,29} seems warranted. We found that RV function was abnormal in the majority of SCD patients with biventricular enlargement in the absence of myocardial scars. This has not been previously reported in studies using echocardiography, a modality that relies on good operator technique and acoustic windows to ensure adequate image quality and which has limited accuracy in quantification of the right ventricle. Pulmonary artery hypertension is a potentially deadly complication in SCD^{30,31} and warrants early recognition, particularly as potentially useful therapies for this condition emerge.^{32,33} In other populations at risk of pulmonary hypertension, resting pulmonary artery pressures may be normal but RV function may be abnormal,³⁴ suggesting that RV dysfunction may precede overt pulmonary hypertension. Reliance on one RV systolic pressure estimate with a supine resting echocardiogram may underestimate the prevalence of pulmonary artery hypertension, as evidenced in this cohort in which more patients had abnormal RV ejec-

tion fraction than elevated RV systolic pressure. By identifying previously unrecognized RV dysfunction, cardiac magnetic resonance imaging may be helpful in determining which SCD patients are at high risk of pulmonary hypertension and allow earlier detection and treatment of this often fatal complication. Ongoing development of serological markers such as brain natriuretic peptide levels to detect subclinical RV dysfunction may lead to the complementary use of such markers along with direct RV quantification with imaging;³⁵ presently, non-cardiac pathologies such as pulmonary thromboembolic disease limit the specificity of the markers.

Transfusion-related myocardial iron overload has been well-described in patients with thalassemia, and may occur in the absence of significant hepatic iron overload.^{9,36} Timely recognition of myocardial iron overload facilitates institution of chelation therapy which can prevent or reverse this form of cardiomyopathy.³⁷ Cardiac magnetic resonance imaging is uniquely able to accurately quantify myocardial iron, which correlates poorly with serum ferritin level, making it an essential tool in improving the understanding of the natural history of thalassemia patients.³⁸ The absence of myocardial iron in this cohort, despite significant hepatic iron overload, was notable. The results of our study were consistent with those of previous studies that have demonstrated myocardial sparing of iron overload in SCD.³⁹ Very limited results from invasive coronary angiographic studies suggest infrequent coronary artery stenoses in SCD patients.^{4,14} Distinctly different pathways of therapy, based on the presence or absence of coronary artery obstruction, underscores the need to define the epicardial coronary artery anatomy in patients presenting with chest pain, which can now be done noninvasively using multi-detector row computed tomography.⁴⁰⁻⁴³ Use of an isotonic contrast agent ensures the safety of this procedure in sickle cell patients.⁴⁴ Investigated with a technique with a reported sensitivity of 95-99%, our cohort had no epicardial coronary artery disease.

Patients with SCD frequently present for evaluation of chest pain of unclear etiology as part of their sickle cell crisis. The relationship of this pain to myocardial

ischemia and coronary artery disease in adults with SCD is unknown. While the study was not designed to assess myocardial perfusion during crises, the findings do suggest that there may be microvascular abnormalities accounting for chest pain in sickle cell patients. The clinical focus in the acute care of these patients typically involves detection of acute chest syndrome and other pulmonary etiologies of chest pain rather than myocardial ischemia. Recognition of microvascular perfusion abnormalities in the acute setting might motivate use of proven ischemia-relieving therapies, such as nitrates, in addition to the narcotic analgesics typically used to relieve pain in this population. Further investigations utilizing the diagnostic strategies demonstrated in this work are needed to define the prevalence of microvascular disease in the acute setting as well as to demonstrate the efficacy of traditional ischemia-relieving therapies in reversing perfusion abnormalities in sickle cell patients.

In summary, we found that a subset of adult SCD patients has myocardial ischemia that occurs in the absence of epicardial coronary artery disease, myocardial infarction or myocardial iron overload. Further studies are ongoing to correlate perfusion abnormalities with chest pain, myocardial ischemia-based therapies, and acute evaluation during crises. Identification of abnormalities in right ventricular function in SCD patients warrants further investigation in risk stratification for pulmonary hypertension and its attendant complications.

SVR designed the research, analyzed images, analyzed data and wrote the manuscript; OPS helped design the imaging protocols in the study, critically reviewed and approved the final version of the manuscript; SRC and EHK took part in the design of the study, enrolled patients, critically reviewed the manuscript and approved its final version. The authors declare that they have no potential conflict of interest.

We thank Beth McCarthy and Valerie Mann-Giles for their assistance in the coordination of the clinical studies and data collection. This work was funded by the State of Ohio Biomedical Research and Technology Transfer Trust Fund grant #02-0022.

Manuscript received June 6, 2006. Accepted August 1, 2006.

References

1. Stuart MJ, Nagel RL. Sickle-cell disease. *Lancet* 2004;364:1343-60.
2. Lonergan GJ, Cline DB, Abbondanzo SL. Sickle cell anemia. *Radiographics* 2001;21:971-94.
3. Wang H, Laslett LJ, Richman CM, Wun T. Acute myocardial infarction in hemoglobin SC disease. *Ann Hematol* 2004;83:622-4.
4. Sherman SC, Sule HP. Acute myocardial infarction in a young man with sickle cell disease. *J Emerg Med* 2004; 27:31-5.
5. Panting JR, Gatehouse PD, Yang GZ, Grothues F, Firmin DN, Collins P, et al. Abnormal subendocardial perfusion in cardiac syndrome X detected by cardiovascular magnetic resonance imaging. *N Engl J Med* 2002; 346:1948-53.
6. Berezowski K, Mautner G, Roberts W. Scarring of the left ventricular papillary muscles in sickle-cell disease. *Am J Cardiol* 1992;70:1368-40.
7. Gerry J, Bulkley B, Hutchins G. Clinicopathologic analysis of cardiac dysfunction in 52 patients with sickle cell anemia. *Am J Cardiol* 1978;42:211-6.
8. Skjaerpe T, Hatle L. Noninvasive estimation of systolic pressure in the right ventricle in patients with tricuspid regurgitation. *Eur Heart J* 1986;7:704-10.
9. Anderson LJ, Holden S, Davis B, Prescott E, Charrier CC, Bunce NH, et al. Cardiovascular T2-star (T2*) magnetic resonance for the early diagnosis of myocardial iron overload. *Eur Heart J* 2001;22:2171-9.
10. Nagel E, Lorenz C, Baer F, Hundley WG, Wilke N, Neubauer S, et al. Stress cardiovascular magnetic resonance: consensus panel report. *J Cardiovasc Magn Reson* 2001;3:267-81.
11. Kellman P, Epstein FH, McVeigh ER.

- Adaptive sensitivity encoding incorporating temporal filtering (TSENSE). *Magn Reson Med* 2001;45:846-52.
12. Simonetti OP, Kim RJ, Fieno DS, Hillenbrand HB, Wu E, Bundy JM, et al. An improved MR imaging technique for the visualization of myocardial infarction. *Radiology* 2001; 218: 215-23.
 13. Flohr TG, Stierstorfer K, Ulzheimer S, Bruder H, Primak AN, McCollough CH. Image reconstruction and image quality evaluation for a 64-slice CT scanner with z-flying focal spot. *Med Phys* 2005;32:2536-47.
 14. Martin CR, Johnson CS, Cobb C, Tatter D, Haywood LJ. Myocardial infarction in sickle cell disease. *J Natl Med Assoc* 1996;88:428-32.
 15. Martin C, Cobb C, Tatter D, Johnson C, Haywood J. Acute myocardial infarction in sickle cell anemia. *Arch Int Med* 1983;143:830-1.
 16. Assanasen C, Quinton RA, Buchanan GR. Acute myocardial infarction in sickle cell anemia. *J Pediatr Hematol Oncol* 2003;25:978-81.
 17. McCrohon JA, Moon JCC, Prasad SK, McKenna WJ, Lorenz CH, Coats AJS, et al. Differentiation of heart failure related to dilated cardiomyopathy and coronary artery disease using gadolinium-enhanced cardiovascular magnetic resonance. *Circulation* 2003;108:54-9.
 18. Kim RJ, Fieno DS, Parrish TB, Harris K, Chen EL, Simonetti O, et al. Relationship of MRI delayed contrast enhancement to irreversible injury, infarct age, and contractile function. *Circulation* 1999;100:1992-2002.
 19. Abdel-Aty H, Zagrosek A, Schulz-Menger J, Taylor A, Messroghli D, Kumar A, et al. Delayed enhancement and T2-weighted cardiovascular magnetic resonance imaging differentiate acute from chronic myocardial infarction. *Circulation* 2004;109:2411-6.
 20. Aessopos A, Tsironi M, Vassiliadis I, Farmakis D, Fountos A, Voskaridou E, et al. Exercise-induced myocardial perfusion abnormalities in sickle beta-thalassemia: Tc-99m tetrofosmin gated SPECT imaging study. *Am J Med* 2001; 111:355-60.
 21. Maunoury C, Acar P, de Montalembert M, Sidi D. Myocardial perfusion in children with sickle cell disease. *Am J Cardiol* 2003;91:374-6.
 22. Acar P, Sébahoun S, de Pontual L, Maunoury C. Myocardial perfusion in children with sickle cell anaemia. *Pediatr Radiol* 2000;30:352-4.
 23. de Montalembert M, Maunoury C, Acar P, Brousse V, Sidi D, Lenoir G. Myocardial ischaemia in children with sickle cell disease. *Arch Dis Child* 2004;89:359-62.
 24. Batra AS, Acherman RJ, Wong WY, Wood JC, Chan LS, Ramicone E, et al. Cardiac abnormalities in children with sickle cell anemia. *Am J Hematol* 2002; 70:306-12.
 25. Balfour I, Covitz W, Davis H, Rao P, Strong W, Alpert B. Cardiac size and function in children with sickle cell anemia. *Am Heart J* 1984;108:345-50.
 26. Moyssakis I, Tzanetea R, Tsafaridis P, Rombos I, Papadopoulos DP, Kaloty-chou V, et al. Systolic and diastolic function in middle aged patients with sickle beta thalassaemia. An echocardiographic study. *Postgrad Med J* 2005; 81:711-4.
 27. Castro O, Hoque M, Brown BD. Pulmonary hypertension in sickle cell disease: cardiac catheterization results and survival. *Blood* 2003;101:1257-61.
 28. Grothues F, Moon JC, Bellenger NG, Smith GS, Klein HU, Pennell DJ. Interstudy reproducibility of right ventricular volumes, function, and mass with cardiovascular magnetic resonance. *Am Heart J* 2004;147:218-23.
 29. Raman S, Cook S, McCarthy M, Ferketich A. Usefulness of multi-detector row computed tomography to quantify right ventricular size and function in adults with either tetralogy of Fallot or transposition of the great arteries. *Am J Cardiol* 2005;95:683-6.
 30. Gladwin MT, Sachdev V, Jison ML, Shizukuda Y, Plehn JF, Minter K, et al. Pulmonary hypertension as a risk factor for death in patients with sickle cell disease. *N Engl J Med* 2004;350:886-95.
 31. Castro O, Gladwin MT, Sachdev V, Jison ML, Shizukuda Y, Plehn JF, et al. Pulmonary hypertension in sickle cell disease: mechanisms, diagnosis, and management of pulmonary hypertension as a risk factor for death in patients with sickle cell disease. *Hematol Oncol Clin North Am* 2005; 19:881-96.
 32. Machado RF, Martyr S, Kato GJ, Barst RJ, Anthi A, Robinson MR, et al. Sildenafil therapy in patients with sickle cell disease and pulmonary hypertension. *Br J Haematol* 2005; 130:445-53.
 33. Reiter CD, Gladwin MT. An emerging role for nitric oxide in sickle cell disease vascular homeostasis and therapy. *Curr Opin Hematol* 2003;10:99-107.
 34. Collins N, Bastian B, Jones C, Morgan R, Reeves G. Abnormal pulmonary vascular responses in patients registered with a systemic autoimmunity database: pulmonary hypertension assessment and screening evaluation using stress echocardiography (PHASE-I). *Eur J Echocardiogr* 2006[in press].
 35. Weber T, Auer J, Eber B. The diagnostic and prognostic value of brain natriuretic peptide and aminoterminal (nt)-pro brain natriuretic peptide. *Curr Pharm Des* 2005;11:511-25.
 36. Tsironi M, Polonifi K, Deftereos S, Farmakis D, Andriopoulos P, Moyssakis I, et al. Transfusional hemosiderosis and combined chelation therapy in sickle thalassaemia. *Eur J Haematol* 2005;75:355-8.
 37. Anderson LJ, Westwood MA, Holden S, Davis B, Prescott E, Wonke B, et al. Myocardial iron clearance during reversal of siderotic cardiomyopathy with intravenous desferrioxamine: a prospective study using T2* cardiovascular magnetic resonance. *Br J Haematol* 2004;127:348-55.
 38. Pennell DJ. T2* Magnetic resonance and myocardial iron in thalassemia. *Ann NY Acad Sci* 2005;1054:373-8.
 39. Wood J, Tyszkaj J, Carson S, Nelson M, Coates T. Myocardial iron loading in transfusion-dependent thalassemia and sickle cell disease. *Blood* 2004; 103:1934-6.
 40. Mollet NR, Cademartini F, Nieman K, Saia F, Lemos PA, McFadden EP, et al. Multislice spiral computed tomography coronary angiography in patients with stable angina pectoris. *J Am Coll Cardiol* 2004;43:2265-70.
 41. Schoenhagen P, Halliburton SS, Stillman AE, Kuzmiak SA, Nissen SE, Tuzcu EM, et al. Noninvasive imaging of coronary arteries: current and future role of multi-detector row CT. *Radiology* 2004;232:7-17.
 42. Kuettner A, Trabold T, Schroeder S, Feyer A, Beck T, Brueckner A, et al. Noninvasive detection of coronary lesions using 16-detector multislice spiral computed tomography technology Initial clinical results. *J Am Coll Cardiol* 2004;44:1230-7.
 43. Raff GL, Gallagher MJ, O'Neill WW, Goldstein JA. Diagnostic accuracy of noninvasive coronary angiography using 64-slice spiral computed tomography. *J Am Coll Cardiol* 2005;46:552-7.
 44. Losco P, Nash G, Stone P, Ventre J. Comparison of the effects of radiographic contrast media on dehydration and filterability of red blood cells from donors homozygous for hemoglobin A or hemoglobin S. *Am J Hematol* 2001;68:149-58.